Applied Energy 285 (2021) 116465

Contents lists available at ScienceDirect

Applied Energy

journal homepage: www.elsevier.com/locate/apenergy

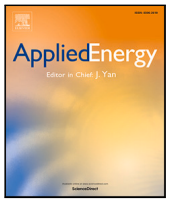

Quantifying resilience in energy systems with out-of-sample testing

Bryn Pickering [a,b,*], Ruchi Choudhary [a,c]

[a] Department of Engineering, University of Cambridge, Cambridge, United Kingdom
[b] Climate Policy Group, ETH Zurich, Zürich, Switzerland
[c] Data-Centric Engineering, Alan Turing Institute, United Kingdom

ARTICLE INFO

Keywords:
District energy systems
Mixed integer linear optimisation
Out-of-sample testing
Resilient systems
Scenario optimisation
Two-stage stochastic programming

ABSTRACT

The need to design resilient energy systems becomes ever more apparent as we face the challenge of decarbonising through reliance on non-dispatchable technologies and sectoral integration. Increasingly, modelling efforts focus on improving system resilience, but fail to quantify the improvements. In this paper, we propose a novel workflow that allows increases in resilience to be measured quantitatively. It incorporates out-of-sample testing following optimisation, and compares the impacts of demand and power interruption uncertainty on both risk-unaware and risk-aware district energy system models. To ensure we encompass the full range of impacts caused by uncertainty, we consider nine distinct objectives encompassing differences in: investment and operation costs, CO_2 emissions, and aversion to risk.

We apply the workflow in a case study in Bangalore, India, and demonstrate that scenario optimisation improves system resilience by one to two orders of magnitude. However, systems designed for resilience to demand uncertainty are not able to gracefully extend to managing risk from extreme shocks to the system, such as power interruptions. We show that shock-induced instability can be addressed by specific measures to reduce grid dependence. Finally, by studying out-of-sample test results, we identify an objective which balances cost, CO_2 emissions, and system resilience; this balance is achieved by novel application of the Conditional Value at Risk measure. These results expose the need for out-of-sample testing whenever uncertainty is considered in energy system modelling, and we provide the framework with which it can be undertaken.

1. Introduction

The design of resilient energy systems is becoming a topic of ever increasing importance [1,2]. In district energy systems, economic risk, regulatory uncertainty, and technology lock-in all weigh on decision makers' choices [3,4]. Accordingly, optimisation model parameters such as demand, weather, and prices are coming under scrutiny for their inherent uncertainty. Sensitivity and scenario analyses are often used to understand the impact of parameter uncertainty in optimisation models, in which a model is rerun multiple times to assess changes in system configuration given variations in one or more parameters. Such analyses can show how future commodity prices might affect the optimal system design [5,6], the relative impact of using measured or simulated weather data to inform renewable technology generation [7], or the ranked effect of many input parameters on the system configuration [8]. However, they cannot be used to design systems with inherent resilience to uncertainty.

More recently, linear optimisation methods which account for uncertainty have been proposed, namely robust optimisation and scenario optimisation (also known as stochastic programming). These methods can be considered as 'risk-aware' optimisation, as opposed to the above-mentioned 'risk-unaware' optimisation. With risk-aware optimisation, the objective is often to converge on capacity deployment which is able to meet demand given any realisation of operational uncertainty. Therefore, the resulting investment could be considered as robust, since it 'expands the set of disturbances a system can respond to effectively' [9].

Risk-aware optimisation models have been used in district and microgrid level studies to incorporate uncertainties across a wide range of parameters including weather, demand, energy supply prices, and operational carbon intensity. Often, several parameters are considered as uncertain in the model. Majewski et al. [10] compared the iterative inclusion of demand, price, and carbon intensity in a robust optimisation model, finding that uncertain demands have the biggest impact on the operational emissions of resulting configurations. Mavromatidis et al. [11], Pazouki and Haghifam [12] also considered three uncertain parameters in their district models: demand, price, and weather. Afzali et al. [13] incorporated demand and prices into a scenario optimisation model in the context of a Chinese building complex. They further added

* Corresponding author at: Climate Policy Group, ETH Zurich, Zürich, Switzerland.
E-mail addresses: bryn.pickering@usys.ethz.ch (B. Pickering), rc488@cam.ac.uk (R. Choudhary).

https://doi.org/10.1016/j.apenergy.2021.116465
Received 6 July 2020; Received in revised form 21 December 2020; Accepted 6 January 2021
Available online 16 January 2021

to the objective function by including risk aversion to CO_2 emissions, finding that expected emissions could be reduced by 8% for a marginal increase in system cost. Demand and weather uncertainty are also frequently considered together, for example in the design of a microgrid in Bolivia [14], a multi-energy district in the UK [15], and for a renewable district generation system in Tokyo [16]. When considering only one uncertain parameter, demand uncertainty is usually the focus [17–20].

Robust optimisation differs from scenario optimisation in that uncertain variables are represented by the extreme extent of their probability distributions. Accordingly, robust optimisation is a more conservative method to bound uncertainty, with limited shapes used to describe these extreme extents [21]; in practice, only the box uncertainty (e.g. +/−10%) is used when applying robust optimisation to energy systems [15,17,22]. Conversely, in scenario optimisation, distinct realisations of uncertain variables are selected. This allows for more complex probability distributions to be described, but it is computationally limited in the number of scenarios that can be considered in parallel; 10–30 scenarios is common [19,23–25]. Having so few scenarios leads to large possible gaps in the uncertainty space. Such gaps can be mitigated by the use of scenario reduction techniques, whereby optimal scenarios are chosen from a much larger set, with the objective to cover as much space of the underlying distributions as possible [12,19,26,27].

An important issue that arises is that even with risk-aware optimisation, it is not immediately apparent how well a solution covers the possible realisations of the future. In scenario optimisation this is because only a subset of possible future scenarios are considered. In robust optimisation, it is common to relax the constraint on strict robustness; some leeway is given for the model to be slightly infeasible for some realisations of uncertainty [10,18]. This means that although a risk-aware system is robust to an expanded set of disturbances, there will be scenarios that were not accounted for in the optimisation. Additionally, the system may be *robust* but not wholly *resilient*. Woods [9] defines four resilience sub-categories, of which 'robustness' is one; 'graceful extensibility' to system shocks is another. Robust designs may not achieve graceful extensibility, failing catastrophically instead when exposed to an unexpected situation. Given that a risk-aware solution is likely to come at a higher investment cost [18] and that the optimisation models of risk-aware energy systems are significantly more expensive computationally, it is reasonable to expect some level of scrutiny to quantify how much better a solution of a risk-aware optimisation is compared to its risk-unaware counterpart.

To quantify the resilience of a solution, Conejo et al. [28] recommends out-of-sample testing as an additional step following risk-aware optimisation. This step requires a modeller to ask the question: 'what happens if we design a system under conditions A, but it undergoes conditions B in operation?', where conditions *A* and *B* are different realisations of uncertainty. Using risk-unaware optimisation, Gabrielli et al. [29] undertook such an analysis for a small district energy system. They analysed 100 system configurations to 1440 realisations of uncertainty, quantifying 'robustness' as a function of demand that could not be met by a configuration; they found that some system configurations were notably more robust than others. Indeed, out-of-sample testing is not only a method to quantify resilience absolutely, it can also inform a modeller how much *more* resilient a risk-aware solution is compared to a risk-unaware solution. Furthermore, it enables the decision-maker to examine the trade-offs associated with having a more resilient system [18]. Finally, and as we will demonstrate later, the out-of-sample tests can be tailored to provide measures of different types of system resilience. While out-of-sample testing can be crucially important to the design of a resilient energy system in the aforementioned manners, it is not yet practised in risk-aware energy system optimisation.

We argue that not only is out-of-sample testing a critical step in justifying the additional cost of risk-aware optimisation, but that a consistent process is required to most benefit from the approach. We test this hypothesis in two parts. As the first step, we compare the optimisation results of risk-unaware and risk-aware formulations for a range of objective functions. The objectives cover the minimisation of monetary costs, carbon emissions, and risk associated with demand uncertainty and power interruptions. By testing a range of typical risk-unaware and risk-aware objective functions, one can quantify variation caused by system design approach relative to the impact of risk awareness in the optimisation. As the second step, we expose the optimisation results to out-of-sample tests to quantify their resilience. Resilience is measured by the sum of hourly imbalance between supply and demand over a year when optimising system operation with a fixed technological configuration.

Although the application of out-of-sample tests is conceptually straightforward, the choice of tests and interpretation of results determines the extent to which an understanding of resilience is acquired. Here, we test for two types of resilience: robustness and graceful extensibility [9]. Robustness to perturbations is tested using stochastic demand profiles and quantified by the variance in energy imbalance across 500 scenarios. Graceful extensibility to system shocks is tested using electricity grid power interruptions and measured by the magnitude of average energy imbalance. To ensure the power interruptions are perceived as a shock to the system, we employ imperfect forecasting [25] in the out-of-sample test optimisation method.

In the following section we describe the illustrative case study, followed by the formulation of the optimisation problem with respect to each objective function (Section 3.1). In the first five objective functions, we do not consider resilience, and therefore only consider different formulations for optimising cost and CO_2 emissions. For the last four objective function formulations, we optimise for resilience of the system by introducing both risk-neutral and risk-averse scenario optimisation. Section 3.2 describes our approach to quantify resilience using out-of-sample tests, in which the resulting system configuration of each objective function is subjected to uncertainty in a rolling horizon optimisation. Optimisation results are presented in Section 4, covering system configurations, incurred monetary costs, and CO_2 emissions. Out-of-sample test results, quantified by system energy imbalance, are presented in Section 5. Finally, we discuss the implications of the results and underlying framework in Section 6.

2. Model and data

A collection of office buildings within Bangalore, India have been selected to define a hypothetical but plausible district. Variants of this fictitious district have been used in previous studies [19,30], so we do not go into detail here on its configuration. Greater detail on the model, including costs and constraint parameters, is available in Section S.1 and in the model online repository.

Fig. 1 shows the nodes used to represent the buildings in the district. Most nodes consist of several buildings, which are connected at the same point on the district cooling network. Building floor area (Table S.1) has been inferred from the external footprint and number of floors for each building. No other information is known about these buildings; we use only their relative size and position to test our modelling approach. The proposed energy centre is on the periphery of the district, sited on a currently undeveloped piece of land, according to satellite data.

Several technologies are allowed at each node (see Tables S.1 and S.2). There is no requirement that a given technology is installed at any particular node, as the investment step of the optimisation will decide this. At a building level, national grid electricity, a diesel generator, and solar photovoltaic panels (PV), are possible technologies to meet electricity demand. In addition to the district cooling system, individual electric chillers can meet cooling demand. In the central energy centre, a more efficient chiller or a combined cooling, heat and power plant (CCHP) can be installed. The CCHP is either a diesel or biomass fuelled generator, whose waste exhaust heat is redirected through an absorption chiller to produce cooling. Thermal energy storage is possible at

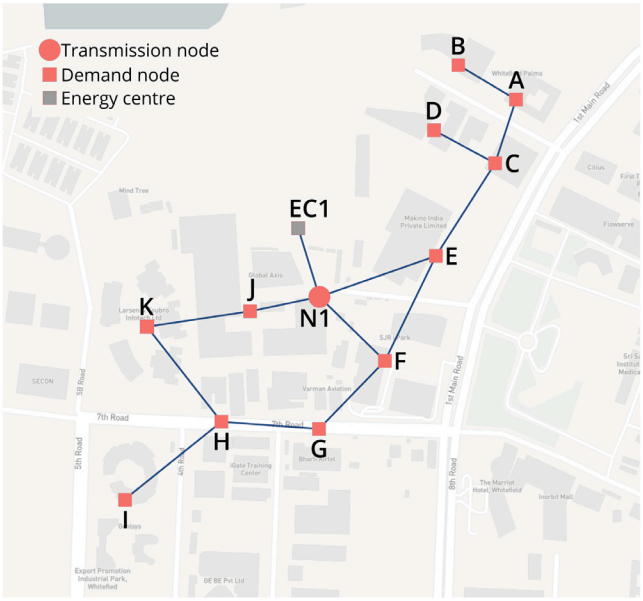

Fig. 1. Bangalore case study district.

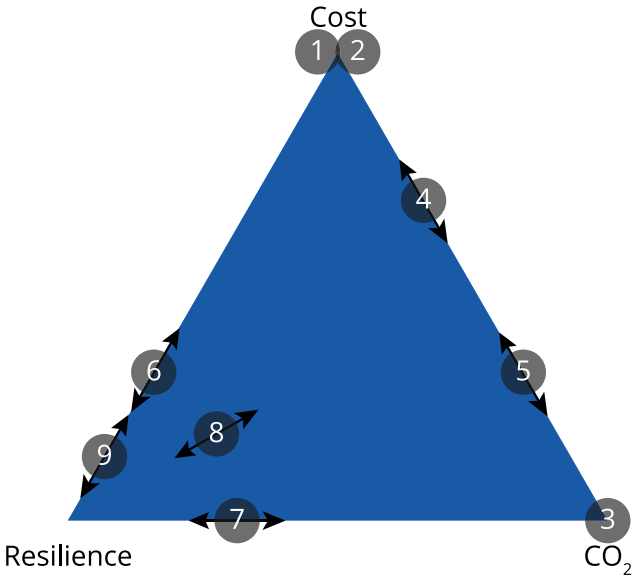

Fig. 2. Graphical representation of the relative importance of each objective class (monetary cost, CO_2 emissions, resilience) considered in this study. Directional arrows depict the ability for weighting parameters to vary the position of the objective within the space. Exact positions of objectives and length of directional arrows are illustrative; they do not represent any particular scale relative to each other.

the energy centre, but due to the relatively low energy density of cold water, we do not consider thermal energy storage at a building level. Electrical battery storage is allowed at all nodes.

Hourly timeseries data in the model includes energy demand derived directly from measured consumption at an office building in Bangalore (discussed further in Section S.3.1.1) and simulated available resource for PV from the Renewables.ninja platform [31]; unlike the demand data, we are unable to validate the PV timeseries against measured data in Bangalore. To maintain tractability, we reduce the length of the time dimension by undertaking timeseries clustering to 12 typical days. To maximise the accuracy of optimisation results following time dimension reduction, we apply the 'masking + clustering' approach [32,33]. Three days are chosen corresponding to maximum electricity demand, cooling demand, and difference between PV resource and electricity demand. The remainder of the timeseries (363 days) is clustered into nine typical days using k-means clustering.

The model is formulated as a mixed integer linear programming (MILP) problem in a modified version of the open-source Calliope v0.6.3 framework [34]. It is subject to various constraints typical to energy system models, which can be found in Section S.2 and within the Calliope framework. Models were run on a high performance computing cluster, with optimisation undertaken by the CPLEX solver (v12.8.1).

3. Methods

3.1. Objective function formulations

To quantify the relative impact of optimising the district energy system for resilience, we consider nine distinct formulations of the objective function. The objectives are formulated to encompass three objective classes: monetary cost, CO_2 emissions, and resilience. It is on these same objective classes that the optimal system configurations will be compared. Five objectives are risk-unaware, the remaining four are risk-aware by implementation of scenario optimisation.

The nine objectives are listed in Table 1 along with the formulation of each objective function. The relative importance of each objective class in the formulations is shown graphically in Fig. 2. Although some objectives focus only on one of cost, CO_2 emissions, or resilience, most are multi-objective problems. Many of the objectives are also able to shift by varying weighting parameters in the objective itself or in an auxiliary constraint. All objective components and auxiliary constraints are summarised in this section; detailed descriptions are given in the supplementary material (Eqs. (S.19), (S.20), (S.24) and (S.25)).

3.1.1. Risk-unaware formulations (Objectives 1 to 5)

In the most basic risk-unaware formulation (Objective 1), the objective function consists of two components: operation cost ($cost^{op}$: Eq. (S.20)) and investment cost ($cost^{inv}$: Eq. (S.19)). All costs which vary with time are considered as operational costs, including those arising from energy production, energy consumption, and energy export. To represent revenue, a negative cost parameter can be applied. Investment costs are those made before beginning operation and are independent of time. These costs arise from the purchase of technologies and may be a function of technology capacity, or may be a fixed quantity applied if any capacity has been installed. To simulate the balance between investment and operational costs over the lifetime of the technologies, given that the model only covers one year, all costs are annualised and discounted to $t = 0$.

Secondary objectives can be included as auxiliary constraints which change the objective function in a linear manner. This method is frequently used in linearised multi-objective optimisation and is referred to as the ϵ-constraint method [e.g.35–37]. Here, we apply this method to (a) minimise operational costs while limiting investment costs (Objective 2), (b) minimise monetary costs while maintaining low CO_2 emissions (Objective 4), and (c) to minimise CO_2 emissions while limiting investment costs (Objective 5).

Eq. (1) gives the generic form of the ϵ constraint. Varying the magnitude of ϵ allows a range of optimal solutions to be calculated, each describing the trade-off between the primary objective and the secondary, ϵ-constrained objective. A decision variable var represents investment cost or CO_2 emissions, and is constrained relative to a baseline value (such as the value obtained for var when there is no ϵ constraint). For clarity, our out-of-sample analysis compares results using only two values of ϵ in each objective, to encompass upper and lower bounds on secondary objectives. The result of iteratively increasing ϵ from a lower to an upper bound is given in the supplementary

Table 1
Summary of objective functions applied in this study, constructed from objective components described in Eqs. (S.19), (S.20), (S.22) and (S.24) and subject to constraints described in Eqs. (1) and (S.25). LL = lost load decision variable, $CVaR$ = conditional value at risk, CoC = cost of carbon.

	Description	Minimise	Subject to
1	Discounted lifetime cost	$cost^{inv} + cost^{op}$	–
2	Operation cost with ϵ-constrained investment	$cost^{op}$	$\epsilon_{cost^{inv}}$
3	CO_2 emissions	CO_2	–
4	Discounted lifetime cost with ϵ-constrained CO_2 emissions	$cost^{inv} + cost^{op}$	ϵ_{CO_2}
5	CO_2 emissions with ϵ-constrained investment	CO_2	$\epsilon_{cost^{inv}}$
6	Risk averse discounted lifetime monetary cost	$cost^{inv} + \sum_{s'} W_{s'} (cost^{op} + LL) + CVaR$	$CVaR^{constr}_{cost^{inv}+cost^{op}+LL}$
7	Risk averse CO_2 emissions	$\sum_{s'} W_{s'} (CO_2 + LL) + CVaR$	$CVaR^{constr}_{CO_2+LL}$
8	Discounted lifetime cost with CO_2 emissions risk aversion	$cost^{inv} + \sum_{s'} W_{s'} (cost^{op} + LL) + CVaR$	$CVaR^{constr}_{CoC*CO_2+LL}$
9	Discounted lifetime cost with grid reliance risk aversion	$cost^{inv} + \sum_{s'} W_{s'} (cost^{op} + LL) + CVaR$	$CVaR^{constr}_{cost^{op}_{x=grid}}$

material.

$$\epsilon^{constr}_{var} \; : \; var \leq \epsilon \times var^{baseline} \tag{1}$$

3.1.2. Risk-aware formulations (Objectives 6 to 9)

Risk-aware optimisation is implemented in a three-step scenario optimisation method with the aim of increasing resilience to time-varying stochastic energy demand profiles [19]. The three steps are: scenario generation, scenario reduction, and scenario optimisation. Scenario generation is used to sample probability density functions describing electricity and cooling demand, generating 500 stochastic demand profiles for each office building in the district. A MILP model optimising across 500 scenarios would be intractable, therefore 16 representative scenarios are selected from the initial set of 500, using scenario reduction. Both scenario generation and scenario reduction are further detailed in Section S.3.1. Once scenarios have been selected, scenario optimisation is undertaken to find a resilient technology portfolio, in light of uncertainty. We extend the scenario optimisation method further in this study to consider risk aversion using the conditional value at risk (CVaR), as detailed hereafter.

In our scenario optimisation model, each scenario describes a different realisation of energy demand. To meet these different demand profiles, timeseries decision variables are optimised independently for each scenario. The expected value of timeseries decision variables is the weighted sum across all scenarios; weights ($W_{s'}$) are assigned according to a scenario's probability of realisation. Time-invariant, investment decision variables are selected before uncertainty is considered, and are therefore independent of scenarios. The resulting objective function (Eq. (2)) is often referred to as risk-neutral, two-stage stochastic optimisation [e.g.11,13,14,26].

$$\min \left(\mathbf{cost^{inv}} + \sum_{s'} W_{s'} \times \mathbf{cost^{op}_{s'}} \right) \tag{2}$$

Risk aversion requires that those scenarios which will have a greater adverse impact on the objective function value are disproportionately weighted; i.e. they are given greater importance than their probability of occurrence would suggest. An additional component is required in the objective to specifically penalise low probability, high risk scenarios. There are many ways of modelling risk-aversion components, including minmax regret, the Hurwicz criterion, value-at-risk (VaR) and conditional value at risk (CVaR) [11]. In this study, we use the CVaR (Eq. S.24)) to implement risk-averse scenario optimisation. The CVaR describes the sum of the expected cost above a given confidence level $\alpha \in [0, 1)$ in the probability distribution which describes all scenarios. As it concentrates on the right-hand tail of the distribution, it is a risk measure that is only influenced by the worst-case scenarios. The strength of risk aversion is dictated by the β multiplier, where $\beta = 0$ corresponds to the risk-neutral scenario optimisation model; several levels of risk aversion are modelled in Objectives 6 to 9.

The 'cost' to which a decision maker is averse does not need to be the same as that given in the primary objective. For example, a system can be minimised against monetary cost, but be risk averse to CO_2 emissions. We implement this secondary objective aversion in the CVaR component of the objective function. This extension of risk-averse scenario optimisation in district energy system optimisation is an additional novel contribution presented in this paper. In this study, we consider risk aversion to (a) operational cost ($cost^{op}$) [objective 6], (b) emissions (CO_2) [objective 7 and 8], and (c) the total cost of electricity purchased from the electricity grid ($cost^{op}_{x=grid}$) [objective 9]. Emissions are monetised using the cost of carbon (CoC), which we set to the highest expected cost applicable to India of 9.49 Indian Rupees (INR)/kgCO_2 [38]. The choice of secondary objective is given in the CVaR subscript in Table 1.

To ensure feasibility across all scenarios and to allow small deviations from feasibility in low probability models, we introduce lost load in the objective function. Lost load is the energy demand not met by the system and is often a variable in microgrid analysis [39,40]. The value of lost load is usually associated with the cost of meeting demand by replacement energy sources [40,41], but this ignores the lack of infrastructure in place to meet that load. Accordingly, we use a relatively large value of lost load of 10^5 INR/kWh or 1 kgCO_2/kWh, which has no physical significance. This large value ensures that lost load is not the 'go to' option for the optimisation, but leaves it open for use [19,29], particularly in low probability scenarios, since the impact of costs on the objective function is proportional to the probability.

3.2. Out-of-sample tests

It is not possible to assess the improvement in system resilience which is realised by incorporating risk in the objective function without applying out-of-sample tests. For the out-of-sample tests we fix technology capacities, given the results of optimising each of the nine objective functions. These fixed capacity systems are then exposed to new operating conditions to evaluate their performance. The new operating conditions are stochastically generated scenarios of uncertain demand and unreliable grid electricity; they are largely independent to those scenarios used for optimisation models (Objectives 6 to 9). Uncertain demand is derived from the 500 generated scenarios described in Section S.3.1.1. Unreliable grid electricity is derived from historic power interruptions in Bangalore, as published by the utility provider for the city. In this section we further describe the methodology for modelling unreliable grid electricity. We also describe the rolling horizon optimisation method used in the out out-of-sample tests, and define the metrics used for quantifying resilience.

3.2.1. Unreliable grid electricity

Power supply interruptions represent shocks to an energy system which can lead to catastrophic failure of energy supply. National grid power interruptions can be a daily occurrence in parts of India [42]. Indeed, the World Bank's Enterprise Surveys show that 46% of electricity consumed by businesses in India is supplied by auxiliary backup generators. Until recently, the local utility provider for the city of Bangalore (BESCOM) maintained and published an unscheduled power outage database which identified the many areas of Bangalore which

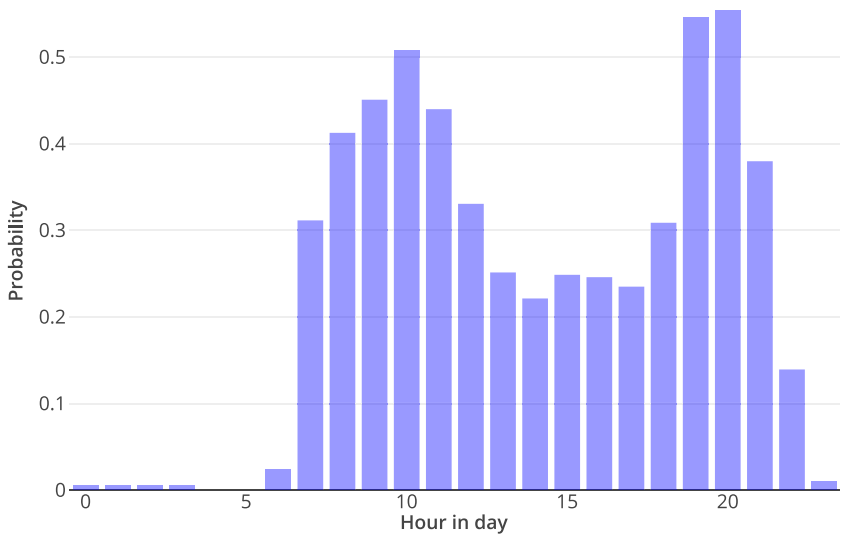

Fig. 3. Distribution of sampled power interruptions based on historical unscheduled interruption data in Bangalore. Each bar represents the probability of power interruption in a given hour of the day.

experience almost daily, unexpected power interruptions caused by load-shedding[1]. Analysing this database, it is apparent that there is a great deal of uncertainty regarding how many distinct interruptions will take place, when they will occur, and for how long.

Using the recorded power outage periods in Bangalore from December 2014 to July 2015, we have constructed a two-part probabilistic representation of power interruptions, which we sample to generate a timeseries for the out-of-sample tests. First, for every day in the year, there is a 70% chance of an outage. Second, for those days randomly selected as having an outage, the start and duration of the morning period (00:00 to 11:59) and the afternoon period (12:00 to 23:59) outages are randomly sampled from lognormal distributions describing the input data. An outage in a twelve hour period n can encroach on the next twelve hour period, $n+1$, if the start time and duration lead to that. However, a sampled outage may not continue into the period $n+2$, as that suggests sampling from a distribution tail which does not exist in the data.

An example of the distribution of sampled interruptions is given in Fig. 3. In this example there is more than 50% chance that an interruption will occur around 10 am and between 7–8 pm. The probability reduces drastically overnight, and is somewhat lower in the middle of the day. This profile of interruptions is consistent with the shape of electricity consumption in the state, as periods of high consumption are more likely to lead to load-shedding.

3.2.2. Rolling horizon optimisation

An energy system optimisation model is typically executed with perfect knowledge of the value of parameters in every time step, even when multiple scenarios are considered. In actual operation, such knowledge of parameters is not possible. Instead, it is only reasonable to expect clarity on operational parameters with a few days of foresight, or even less when shocks to the system take place.

By fixing technology capacities based on the optimal technology portfolio, a model can be run using a 'rolling horizon' to emulate this state of limited knowledge. Although optimisation will take place for the full time series, it is done in smaller chunks of a few days, with each chunk being the scheduling horizon. Optimisation is run over each horizon, with the intent of implementing only a sub-period: the scheduling window. The period between the end of the window and the end of the horizon is considered a 'forecast'. It is only used to provide a trajectory for the scheduling window.

As can be seen in Fig. 4, the horizon will ultimately become the window, as the optimisation steps through time. With perfect foresight (Fig. 4, step 2a), the parameter values do not change when moving from the scheduling horizon to the scheduling window. Instead, to emulate imperfect forecasting, the horizon can be given different parameter values to those seen in the window, for the same time steps (Fig. 4, step 2b). Existing studies have considered both perfect and imperfect forecasting. Where uncertainty has been introduced, it has included pricing [43,44], weather [25,44,45], and demand [43,46,47]. In the perfect foresight case, there is redundancy in the optimisation; only the results from the scheduling window are actually retained. Nevertheless, the computational time is small relative to optimising an entire year in one go, as linear programming algorithms tend towards solving in a polynomial time, relative to their size [48]. In this study, we used a 24 h horizon and a 12 h window.

Perfect foresight was assumed when only considering 500 new demand scenarios in the out-of-sample tests. A power interruption profile is then overlaid onto each of these 500 demand scenarios, to quantify the relative change in system resilience. As discussed in Section 3.2.1, this intermittency is based on recorded data of unexpected power interruptions in Bangalore, India. Using the two-part probabilistic representation, the intermittency in each day of the year is sampled independently, creating an annual profile of power interruptions to be applied in the rolling horizon optimisation. Given that unreliable grid electricity is an unexpected component of an energy system, the interruptions are applied using an imperfect forecast. In the scheduling horizon, electricity supply is deemed to be reliable (i.e. infinitely available); only in the scheduling window are the interruptions introduced. In these interrupted periods, the availability of grid electricity effectively changes from infinite to zero.

3.2.3. Defining resilience

We distinguish in this study between resilience as a measure of *robustness* or *graceful extensibility*, defined by Woods [9] as resilience ⟨2⟩ and ⟨3⟩, respectively. A robust system is one which 'expands the set of disturbances a system can respond to effectively' [9]. Invariance in a particular sense Z when perturbations of type Y are applied ensures robustness [49]. This requirement for knowledge of the perturbations and the sense of variability means that robustness is defined quite narrowly.

[1] At the time of publishing, the database was no longer publicly accessible.

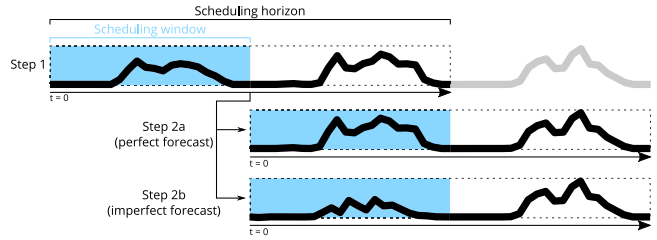

Fig. 4. Depiction of a rolling horizon optimisation, where decisions are made in step 1 for the scheduling window, considering an optimisation over the scheduling horizon. Step 2 constitutes a step forward in time, and another optimisation. Steps 2a and 2b show the realisation of a perfect and imperfect forecast, respectively.

Unlike the definition of robustness, which measures invariance across a particular known uncertainty set, graceful extensibility is a measure of system brittleness [9]. Indeed, even if variance in out-of-sample tests can be kept low to ensure robustness, resulting systems can still fail catastrophically when exposed to the realisation of unknown uncertainty in system parameters [9,50]. The main goal of a gracefully extensible resilient system is to not be susceptible to catastrophic failure, even if this means great deviation from a pre-defined objective function.

In this study, resilience is quantified by the annual system energy imbalance and it is calculated in each out-of-sample test. The lost load introduced in Section 3.1.2 is used to capture the inability for the investment to balance supply and demand, whether due to under-production leading to unmet demand or over-production leading to excess supply. The latter imbalance would be caused by non-dispatchable rooftop PVs producing electricity that cannot be exported, or the CCHP load-following electricity demand, but overproducing cooling energy in the process. The absolute values of over- and under-production are combined to give the total energy imbalance for a test. The variance and magnitude of this imbalance can be separated to better understand the measure of resilience ⟨2⟩ and ⟨3⟩. Low variance indicates a robust system, while a low maximum magnitude indicates graceful extensibility.

4. Optimisation results

Fig. 5 provides an overview of monetary cost, CO_2 emissions, and technology portfolio associated with the optimal result for each objective function. Results for upper and lower bounds of ϵ and β are given here, for ϵ-constrained and risk-averse objectives, respectively. Results pertaining to intermediate values of ϵ and β are given in Section S.4. In this section, we discuss the results from each variation of the objective function given in Fig. 5.

4.1. Risk-unaware objectives

Most energy system optimisation models are formulated to minimise discounted lifetime cost (Objective 1). For our particular example, no district-scale system is installed when Objective 1 is applied (Fig. 5b). Nevertheless, investment does take place in PV and battery storage, neither of which are commonly used to meet demand in Bangalore; the PV capacity corresponds to use of only one third of the available rooftop area in the district. As expected, Fig. 5a shows that Objective 1 has the lowest discounted lifetime cost, but there are many scenarios with both higher and lower CO_2 emissions.

By applying an objective that minimises investment cost, investment costs can be reduced by approximately 70% compared to when minimising discounted lifetime cost (Table 2). This results in an elimination of investment in PV and battery storage. There is nowhere near the same scope to reduce operation cost, with only a 2% reduction in operating costs when allowing investment costs to double. This minor reduction is predicated on investment in a district-scale energy centre, with a energy centre chiller producing cooling.

Table 2
Comparison of optimal investment ($cost^{inv}$) operation cost ($cost^{op}$), and CO_2 emissions (CO_2) between Objectives 1, 2 and 3; for further information on objective numbers, see Section 3.

	$cost^{inv}$	$cost^{op}$	CO_2
min(cost) (Objective 1)	5.00×10^7	2.89×10^8	2.53×10^7
min($cost^{op}$) (Objective $2_{\epsilon=2}$)	1.00×10^8 ↑	2.86×10^8 ↓	2.50×10^7 ↓
min($cost^{inv}$) (Objective $2_{\epsilon=0.31}$)	1.56×10^7 ↓	3.66×10^8 ↑	3.2×10^7 ↑
min(CO_2) (Objective 3)	2.76×10^8 ↑	5.21×10^8 ↑	1.90×10^7 ↓

Minimising CO_2 emissions leads to complete independence from grid electricity, in favour of biomass and diesel fuel use. Although diesel generators are often considered as the highly polluting back-up electricity source, in Bangalore they are able to produce electricity with a lower emission factor ($0.63 kgCO_2/kWh_e$) to the national grid ($0.7 kgCO_2/kWh_e$) [51]. Such a high emissions factor for grid electricity (approximately twice that of the UK, for example) is a function of both the state fuel mix and high transmission losses (~13%) [52]. The installed CCHP operates in two modes (see Fig. S.6): as a baseload electricity provider, storing excess thermal energy where necessary, and as a peak electricity provider to allow the thermal storage to discharge. Most electrical requirements are met by building-level diesel generators and relatively minor use is made of battery storage, usually charging at peak PV output and discharging at peak electricity demand, since there is a two to three hour difference between the two peaks.

This grid independence reduces CO_2 emissions by 25%, but results in a doubling of discounted lifetime cost. The cost of technology investment increases by an order of magnitude and the operation cost almost doubles (Table 2). This increase in monetary cost cannot be avoided if CO_2 emissions are to be kept low; minimising lifetime costs subject to constraints on CO_2 emissions provides the identical result to minimising CO_2 emissions directly. Similarly, constraining low investment costs leads to the same result whether minimising operating costs (Objective $2_{\epsilon=0.31}$) or CO_2 emissions (Objective $5_{\epsilon=0.31}$). A compromise solution is found when allowing investment cost to double. Objective $5_{\epsilon=2}$ maintains practically the same low emissions as Objective 3 but discounted lifetime cost is one third lower. This lower cost is possible by lower investment in thermal storage, requiring biomass CCHP to be partially replaced by chillers in meeting cooling demand (Fig. 5b).

Any reasonable cost of carbon is ineffective in light of such large increases in system cost; if a high cost of carbon of 9.49 INR/$kgCO_2$ [38] were applied as part of the discounted lifetime cost minimisation objective, a mere 10% reduction in CO_2 emissions could be realised (see Fig. S.7a). A more 'politically' viable cost of carbon of 0.365 INR/$kgCO_2$ [38] would have no perceptible impact on the CO_2 emissions, nor the investment decision. Indeed, a 2.5% reduction in CO_2 emissions requires a cost of carbon of 7.26 INR/$kgCO_2$.

4.2. Risk-aware objectives

Attempting to increase system resilience has one key effect: an increase in total installed technology capacity (Fig. 5b). The choice of technologies do not change; the same technologies already found in the risk-unaware objective results are found when optimising the system with the corresponding risk-aware objectives. Although capacities increase, expected annual energy production does not change (Fig. 5b). Technology capacity is being purchased with the expectation that technologies will operate with a lower capacity factor. Additional capacity does increase system cost, but by under 10% when introducing scenario optimisation to the minimisation of discounted lifetime cost. This objective also results in an increase in CO_2 emissions of approximately 10%.

CO_2 emissions can be severely reduced by introducing scenario optimisation to the minimisation of emissions, primarily by utilising

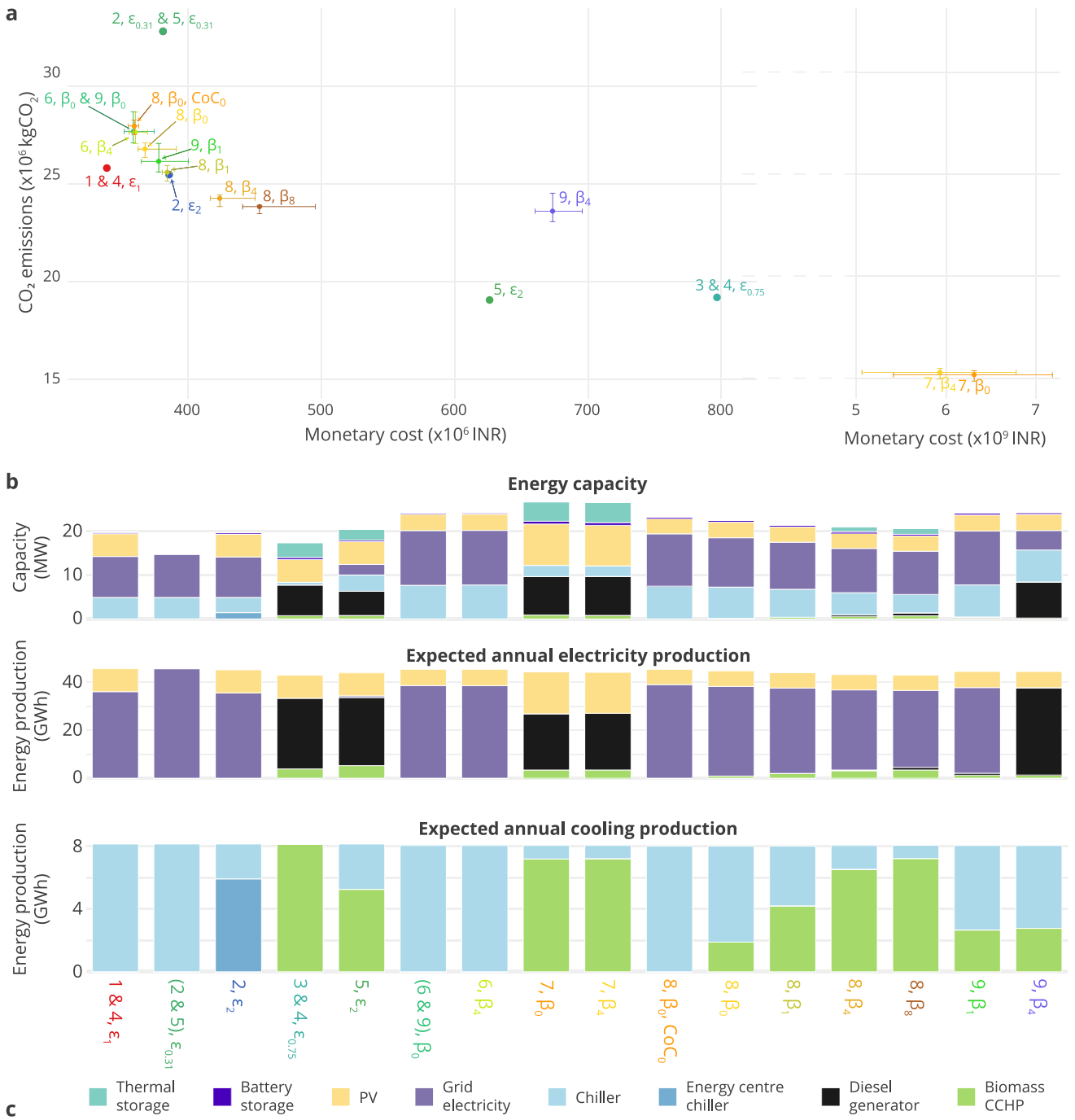

Fig. 5. Overview of results from each variation of the objective function. **(a)** The discounted lifetime monetary cost and operational CO_2 emissions; markers are given for the expected value of SO models, with whiskers defining the extent of possible values associated with individual scenarios. **(b)** Installed technology capacity, expected annual electricity production, and annual cooling energy production; alternating grey/white backgrounds highlight changes in objective. **(c)** Description of objective number; for more information refer to Section 3. Where results overlap, objective numbers have been placed together (e.g. '3 & 4, $\epsilon_{0.75}$' refers to objectives '3' and '4, $\epsilon_{0.75}$' having the same result). For brevity, '(2 & 5), $\epsilon_{0.31}$' in **(b)** is equivalent to '2, $\epsilon_{0.31}$ & 5, $\epsilon_{0.31}$' in **(a)**. Results associated with the upper and lower bounds of ϵ are given for Objectives 1, 2, 4 and 5. Results associated with risk neutral ($\beta = 0$) and risk averse ($\beta > 0$) SO are given for Objectives 6 to 9.

lost load as a mechanism to avoid emissions. This leads to several orders of magnitude increase in system cost, which is a result of the high monetary value of lost load. Monetary cost and CO_2 emissions can be balanced in the scenario optimisation objective function (Objective 8), by placing a 9.49 INR/kgCO_2 cost of carbon in the CVaR objective component. Even when risk neutral, the expected CO_2 emissions of

Table 3
Investment cost for optimal solutions derived from models aimed at improving power interruption resilience by applying grid electricity risk aversion in the scenario optimisation CVaR component (Objective 9). Investment cost for optimal solution of the baseline, risk-unaware model (Objective 1) given for comparison.

	Objective 1	Objective 9		
		$\beta = 0$	$\beta = 1$	$\beta = 4$
$\mathbf{cost}^{inv}$ ($\times 10^7$**INR**)	5.01	4.92	6.32	7.34

Objective 8 are lower than Objective 6 (Fig. 5a). However, CO_2 risk aversion of at least $\beta = 1$ is required to ensure expected CO_2 emissions lower than that realised by Objective 1. With increasing risk aversion, the range of possible operational CO_2 emissions decreases, but the range of monetary costs increases (see also Fig. S.10).

When running the scenario optimisation model to penalise only high dependence on grid electricity (Objective 9), the system quickly becomes autarkic, i.e. it no longer depends on any electricity from the grid. Although there is supposedly some grid electricity capacity at a risk aversion level of $\beta = 4$, actual purchases from the grid are negligible. Instead, building-level diesel generators are the optimal choice.

Aversion to grid electricity does not always lead to an autarkic system. If $\beta = 1$ in Objective 9, grid dependency remains high, with less than 10% of the risk-neutral scenario optimisation grid dependence transferred to diesel generator (diesel generator) or biomass fuelled CCHP production. Implementing the most national grid electricity (grid electricity) averse scenario optimisation objective requires an additional 23 million INR of investment compared to the baseline cost model (Table 3). The cost is incurred by investment in diesel generators in favour of a connection to the electricity grid or access to a centralised energy system. Due to energy autarky being achieved, there is a reduction in expected CO_2 emissions of up to 10% alongside this increase in system cost.

5. Out-of-sample test results

In this section, the out-of-sample tests introduced in Section 3.2 have been applied to each of the nine objectives, to quantify robustness and graceful extensibility of the system under demand variations and grid electricity interruptions. Resilience is measured based on energy imbalance: i.e. the total mismatch between hourly supply and demand over a whole year. This energy imbalance can be caused by both under- and over-production of energy, relative to demand; we do not make a distinction between the value of these two adverse effects. In all tests, we found most of the imbalance to be caused by under-production, which is expected given that an over-producing system must also invest in additional capacity to be in a position to over-produce. Although the value assigned to under- and over-production is likely to be different in practice, we do not make a distinction between the two since we cannot quantify the relative cost of mitigating either undesirable effect at a district scale. We consider a system as more robust if it has a low variance in energy imbalance across all 500 out-of-sample scenarios; graceful extensibility is measured on the maximum energy imbalance across all scenarios. A system which has high levels of energy imbalance and high variance is the least resilient.

5.1. Out-of-sample tests with demand variations

Fig. 6 gives an overview of the cooling and electricity imbalance for each variation of the objective function (Objectives 1 to 9).

Between risk-unaware models, variation in energy imbalance is relatively low. Nevertheless, the imposition of a lower investment cost leads to a lower level of electrical energy imbalance than the discounted lifetime cost model. Conversely, minimising CO_2 emissions leads to a higher electrical energy imbalance, and the highest total energy imbalance of all the objectives. Albeit with similarly low CO_2 emissions, and correspondingly low dependence on grid electricity (Fig. 6b), minimising CO_2 emissions with an allowed doubling in investment costs compared to Objective 1 leads to the lowest total energy imbalance. Such variations in resilience relative to impacts on cost and CO_2 emissions makes it evident that the inherent resilience of risk-unaware objectives cannot necessarily be fathomed prior to running out-of-sample tests.

The introduction of demand uncertainty in the objective function of a model does markedly improve robustness (distribution variance) and graceful extensibility (distribution maximum) to energy imbalance. The risk-unaware objective system configurations are all likely to incur a one or two magnitude greater quantity of energy imbalance than their risk-aware counterparts. Within the scenario optimisation models, the technology portfolio resulting from carbon minimisation leads to a lower cooling energy imbalance than that resulting from cost minimisation; resilience of these two objectives is inverted when considering electrical energy imbalance. Adding a cost of carbon to the risk-aware cost minimisation objective leads to an energy imbalance range that sits between the cost and CO_2 emissions minimisation results. By balancing the two objective classes models, the Objective 8 technology portfolio creates a similar imbalance of cooling and electrical energy.

Risk-aware CO_2 emissions minimisation has a larger variability in energy imbalance between out-of-sample tests than any other model. In the worst case scenarios, electrical energy imbalance can be greater than some of the risk-unaware models. These worst case test results signifies that this technology portfolio is not gracefully extensible, when compared to other risk-aware portfolios.

5.2. Introduction of power interruptions

Fig. 7 gives an overview of the cooling and electricity imbalance for each variation of the objective function tested against power interruptions. Fewer formulations of the objective were tested than in the demand uncertainty out-of-sample tests.

The electrical energy imbalance is similar between Objective 1 and its risk-aware counterpart models, both risk-neutral and risk-averse. Energy imbalance has increased by two and four orders of magnitude for the risk-unaware and risk-aware models, respectively, compared to the demand uncertainty out-of-sample tests undertaken in the previous section. Cooling demand is unaffected, however. As with the previous set of out-of-sample tests, the system configuration resulting from minimising CO_2 emissions with risk awareness leads to a large possible variation in energy imbalance. However, this variation is skewed towards lower levels of imbalance than that given by the expected value.

The impact of reducing grid electricity dependence is exhibited on both electricity and cooling imbalance, with the possibility of reducing both by several orders of magnitude. As the magnitude of error decreases, the error variance also decreases, meaning the expected energy imbalance is more certain. Additionally, using the electrically autarkic $\beta = 4$ grid electricity risk-averse scenario optimisation results, a lower cooling energy imbalance is realised as compared to the original $\beta = 4$ risk-averse scenario optimisation model result shown in Fig. 6.

Given the cost of reducing dependence on national grid electricity (see Table 3) and the resulting reduction in energy imbalance, it is possible to calculate the cost of increased resilience to unmet demand. The additional 23 million INR of investment required to install the most conservative systems corresponds to a cost of 1.9 INR per kWh of avoided unmet demand.

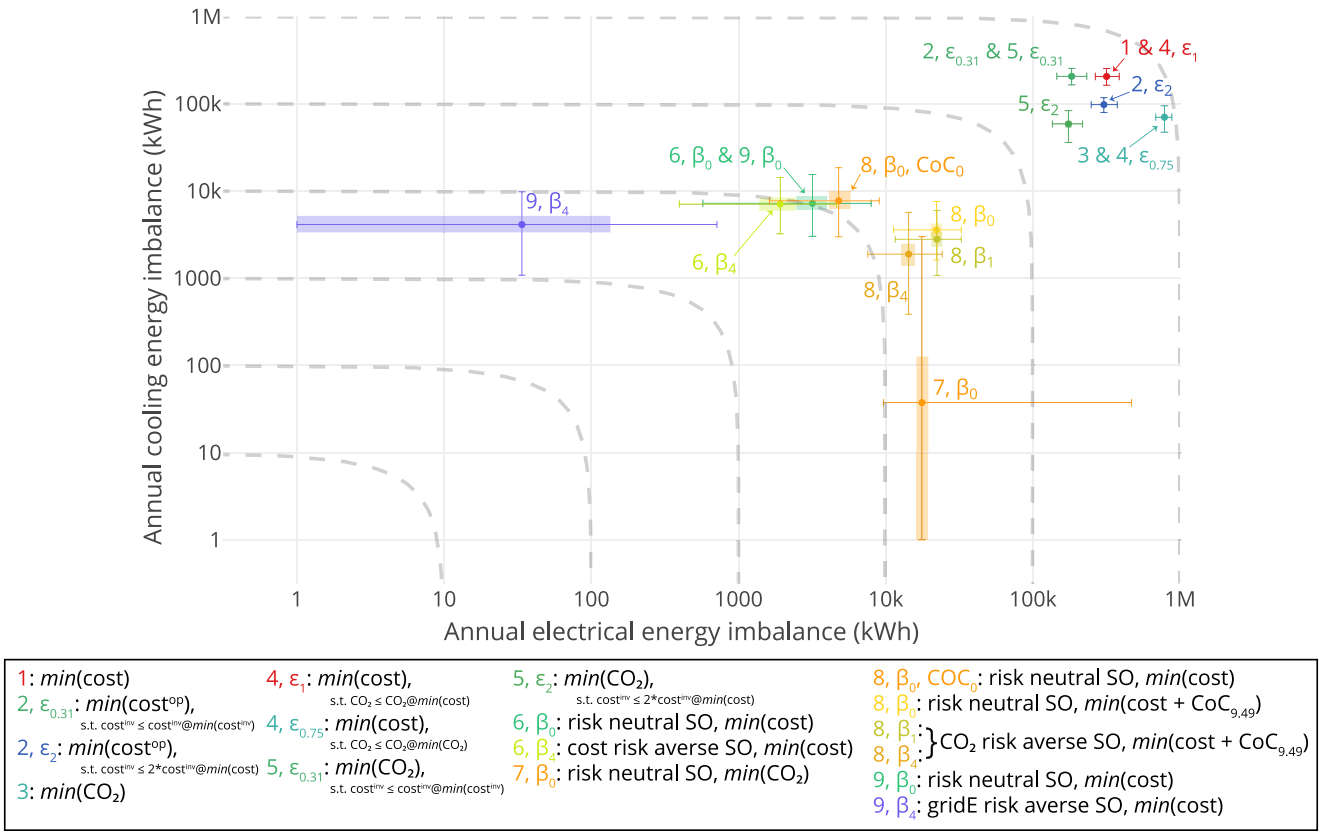

Fig. 6. Overview of electricity and cooling imbalance following 500 out-of-sample tests for each variation of the objective function. Energy imbalance is given as a distribution, with markers showing the median, boxes showing the interquartile range, and whiskers showing the minimum and maximum system energy imbalance for both cooling and electricity. Dashed lines follow constant sums of total energy imbalance. A value of 1 has been given to any value below 1, to ensure readability on the log–log axes. The figure key gives a short description of each objective number; for more information refer to Section 3. Where results overlap, objective numbers have been placed together (e.g. '3 & 4, $\epsilon_{0.75}$' refers to objectives '3' and '4, $\epsilon_{0.75}$' having the same result).

6. Discussion and conclusions

In this paper we have examined the introduction of out-of-sample testing as a method to measure energy system resilience in mixed integer linear programming. To do so, we have optimised the technology investment and operation in a district energy system in the context of Bangalore, India. The system has been optimised according to nine objectives, each of which is compared on expected cost, CO_2 emissions, and resilience to uncertain demand and grid power interruptions. Five of these objectives took no account of uncertainty (risk-unaware objectives), while the other four utilised two-stage scenario optimisation (risk-aware objectives) in an attempt to increase their resilience to uncertain demand.

The use of out-of-sample testing has shown that the optimisation objectives which utilise scenario optimisation do increase system resilience, both in terms of 'robustness' and 'graceful extensibility', as defined by Woods [9]. However, they do not lead to a system which is completely capable of eliminating lost load, where demand for cooling or electricity goes unmet. It is necessary to be aware of these caveats when using risk-aware techniques such as scenario optimisation; it is not sufficient to state that a system is 'resilient' following risk-aware optimisation, a relative measure calculated ex-post is required to determine *how* resilient a system is.

If decision makers are willing to invest in more capacity, they may be able to achieve greater savings in CO_2 emissions and operation cost while also increasing system resilience. In the Bangalore context, centralised cooling provision becomes viable for a relatively small increase in investment cost, presenting a low barrier to influencing a decision maker with auxiliary incentives, such as a decrease in CO_2 emissions. Yet, allowing additional capacity investment relative to an objective of minimising lifetime costs does not automatically confer an improvement in system resilience to energy imbalance. It is necessary to allocate additional capacity sensibly. Indeed, all risk-unaware scenario models have an order of magnitude greater energy imbalance than those which consider risk in the objective, even though some risk-unaware objectives demand an order of magnitude greater investment than risk-aware objectives.

Improving system resilience using scenario optimisation requires, in most cases, only an increase of monetary cost and carbon emissions of around 10%. In the case of minimising CO_2 emissions in the context of scenario optimisation, CO_2 emissions could fall compared to the risk-unaware objective, but the monetary cost would increase by several orders of magnitude due to the over-purchase of PVs and subsequent electricity curtailment. A focus on minimising CO_2 emissions would also be the least helpful in ensuring resilience, as out-of-sample tests indicate a high variability in energy imbalance relative to all other designs (both risk-unaware and risk-aware). These outlier scenarios are unique to this particular objective and are a sign of a system which is neither robust nor gracefully extensible.

If a cost of carbon is used to incorporate carbon into a risk-aware minimisation of discounted lifetime cost, a 9.49 INR/kgCO_2 cost of carbon would lead to a system which compromises on cost, carbon, and resilience. Compared to each objective considered independently, combining cost minimisation with risk awareness and aversion to monetised CO_2 emissions leads to a system with relatively well-balanced monetary cost, carbon emissions, and energy imbalance. Although there is a marginal increase in each objective metric, it is well-balanced compared to the poor performance of the independent objectives in the metrics they did not explicitly consider: CO_2 emissions when minimising cost and monetary cost when minimising CO_2 emissions. This

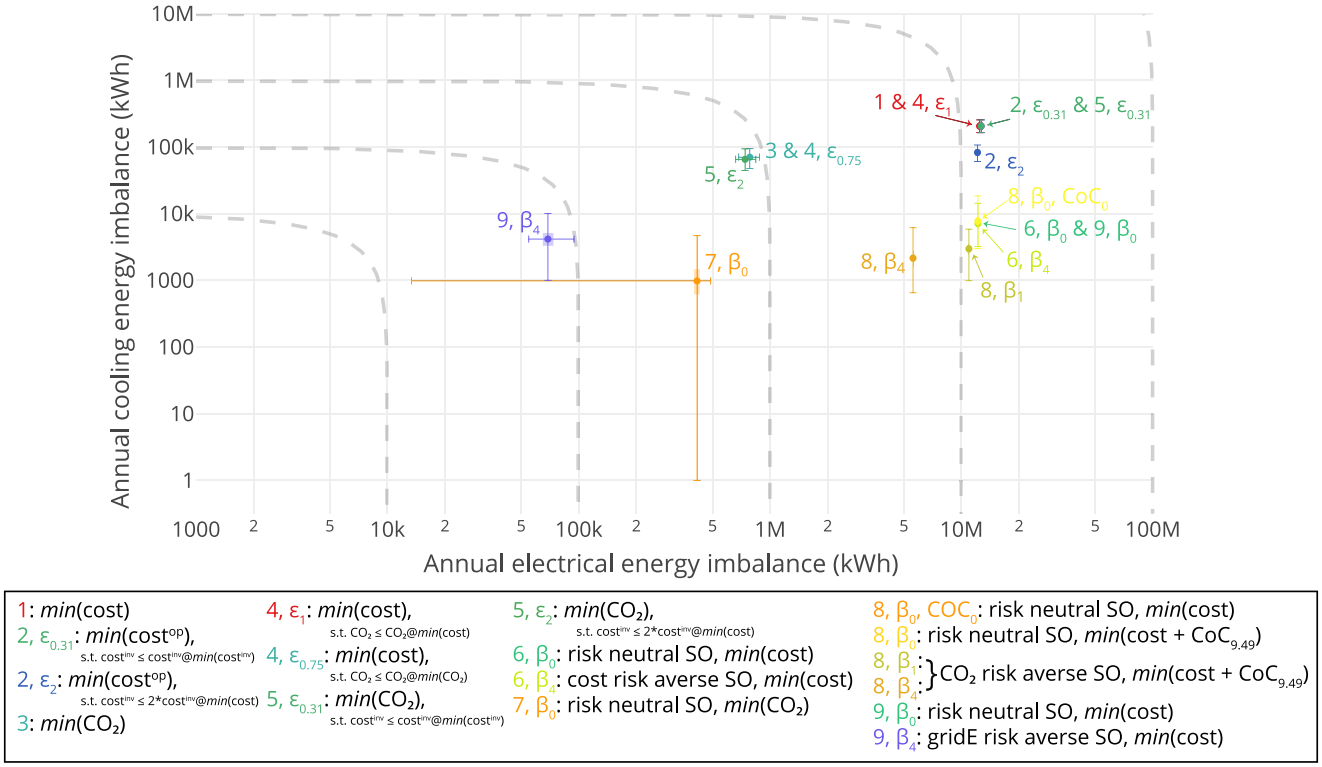

Fig. 7. Overview of electricity and cooling imbalance for each variation of the objective function following 500 out-of-sample tests in which there is uncertain demand and random interruptions to grid electricity. Energy imbalance is given as a distribution, with markers showing the median, boxes showing the interquartile range, and whiskers showing the minimum and maximum system energy imbalance for both cooling and electricity. Dashed lines follow constant sums of total energy imbalance. A value of 1 has been given to any value below 1, to ensure readability on the log–log axes. The figure key gives a short description of each objective number; for more information refer to Section 3. Where results overlap, objective numbers have been placed together (e.g. '3 & 4, $\epsilon_{0.75}$' refers to objectives '3' and '4, $\epsilon_{0.75}$' having the same result).

compromise objective would result in the use of a centralised biomass fuelled CCHP to meet most cooling demand, but would still require heavy dependence on the national grid for electricity.

Of course, such dependence on grid electricity would cause significant system reliability issues if allowing electricity interruptions to be considered. The impact of interruptions on models which do not expect them is much larger than the impact of uncertain demand. Mitigating the effect of power interruptions also leads to a shift in technology choice, but this choice is still averse to district systems, instead preferring building-level diesel generators. This result is more in-keeping with the existing technology choices made for commercial properties in Bangalore, whereby a diesel generator meets grid electricity supply shortfall. Indeed, the building from which demand data was acquired has two diesel generators to handle power interruptions. Resilience to power interruptions is certainly worthwhile, since the impact on energy imbalance is substantial. However, this comes at a considerable increase in the capacity of technologies. This additional investment could be justified if considering it as a cost per unit of mitigated energy imbalance, but this puts pressure on the optimisation results to be realistic, rather than indicative of the relative benefits of objectives. Furthermore, investments in diesel generators should be weighed against their emissions; they are currently favourable in terms of CO_2 emissions but, unlike the grid, there is no scope to reduce these emissions. Diesel generators also impact local air quality, which could be added as another auxiliary objective if studying these particular solutions in more detail [53,54].

Our study of out-of-sample testing in the context of demand uncertainty and grid power interruptions opens many avenues for exploring resilience in energy systems more thoroughly. Uncertainty is not limited to these parameters, nor to this spatial scope. For instance, at the district scale, weather uncertainty [14–16] and energy prices [11,12] are frequently a component of resilient system design. At the national scale, the impact of weather uncertainty is further amplified by the existence of more non-dispatchable technologies than just PV, including wind and hydropower [55,56]. Weather can also cause national system shocks, examples of which include monsoon rainfall [57] and low-wind-power events [58]. Given the number of risks involved across spatial scales, the need for resilient systems is clear and the need to conduct out-of-sample testing is further amplified.

In conclusion, we recommend the use of out-of-sample testing as an additional step in energy system optimisation, when parameter uncertainty is under consideration, and provide the framework with which it can be undertaken. Incorporating resilience in district energy system optimisation makes it possible to better understand system viability and the trade-offs between investment and operation costs, CO_2 emissions, and system resilience to energy imbalance. Using out-of-sample testing applied to a district energy system in Bangalore, India, we demonstrate that scenario optimisation improves system resilience to unmet demand by one to two orders of magnitude. Shocks to the system lead to brittle systems; we show that aversion to national grid dependence markedly mitigates this system brittleness, but at a cost of approximately 1.9 INR/kWh of avoided unmet demand. Moving forward, additional impacts of uncertainty on system design, including weather, price, and emissions intensity, could be incorporated into both the optimisation process and to ex-post analyses. Auxiliary impacts, such as the particulate emissions of diesel generators which provide system resilience in Bangalore when power interruptions occur, could also be assessed to better understand the trade-offs accepted upon incorporating resilience. Both these possible next steps are made possible by the implementation of the process presented in this paper: comparing various objectives, three-step scenario optimisation, and out-of-sample testing.

CRediT authorship contribution statement

Bryn Pickering: Conceptualization, Data curation, Formal analysis, Investigation, Methodology, Software, Validation, Visualization, Writing - original draft, Writing - review & editing. **Ruchi Choudhary:** Methodology, Resources, Supervision, Writing - original draft, Writing - review & editing.

Declaration of competing interest

The authors declare that they have no known competing financial interests or personal relationships that could have appeared to influence the work reported in this paper.

Data availability

The open-source Calliope energy system framework was used to undertake the optimisation and out-of-sample testing for this analysis. All data on the Bangalore case study, including the relevant Calliope model configuration can be found in the model online repository.

Acknowledgements

This research was supported by the Engineering and Physical Sciences Research Council, United Kingdom (reference number: EP/L016095/1) and the Centre for Digital Built Britain, under InnovateUK grant number RG96233. We are also grateful to our demand data providers: the Indian Institute of Human Settlements (IIHS) and the Cambridge University Living Laboratory for Sustainability. This work was performed using resources provided by the Cambridge Service for Data Driven Discovery (CSD3) operated by the University of Cambridge Research Computing Service (http://www.csd3.cam.ac.uk/), provided by Dell EMC and Intel using Tier-2 funding from the Engineering and Physical Sciences Research Council, United Kingdom (capital grant EP/P020259/1), and DiRAC funding from the Science and Technology Facilities Council, United Kingdom (www.dirac.ac.uk).

Appendix A. Supplementary data

Supplementary material related to this article can be found online at https://doi.org/10.1016/j.apenergy.2021.116465.

References

[1] Jesse B-J, Heinrichs HU, Kuckshinrichs W. Adapting the theory of resilience to energy systems: A review and outlook. Energy Sustain. Soc. 2019;9(1):27. http://dx.doi.org/10.1186/s13705-019-0210-7.

[2] Mola M, Feofilovs M, Romagnoli F. Energy resilience: Research trends at urban, municipal and country levels. In: International scientific conference "environmental and climate technologies", Energy Procedia In: International scientific conference "environmental and climate technologies", 2018;147:104–13.http://dx.doi.org/10.1016/j.egypro.2018.07.039,

[3] Hawkey D, Webb J, Winskel M. Organisation and governance of urban energy systems: District heating and cooling in the UK. In: Special issue: advancing sustainable urban transformation, J Cleaner Prod In: Special issue: advancing sustainable urban transformation, 2013;50:22–31.http://dx.doi.org/10.1016/j.jclepro.2012.11.018,

[4] Kelly S, Pollitt M. An assessment of the present and future opportunities for combined heat and power with district heating (CHP-DH) in the United Kingdom. In: Energy Efficiency Policies and Strategies with Regular Papers., Energy Policy In: Energy Efficiency Policies and Strategies with Regular Papers., 2010;38(11):6936–45.http://dx.doi.org/10.1016/j.enpol.2010.07.010,

[5] Wouters C, Fraga ES, James AM. An energy integrated, multi-microgrid, MILP (mixed-integer linear programming) approach for residential distributed energy system planning – a south Australian case-study. Energy 2015;85:30–44. http://dx.doi.org/10.1016/j.energy.2015.03.051.

[6] Yazdanie M, Densing M, Wokaun A. The role of decentralized generation and storage technologies in future energy systems planning for a rural agglomeration in Switzerland. Energy Policy 2016;96:432–45. http://dx.doi.org/10.1016/j.enpol.2016.06.010.

[7] Bracco S, Delfino F, Ferro G, Pagnini L, Robba M, Rossi M. Energy planning of sustainable districts: Towards the exploitation of small size intermittent renewables in urban areas. Appl Energy 2018;228:2288–97. http://dx.doi.org/10.1016/j.apenergy.2018.07.074.

[8] Mavromatidis G, Orehounig K, Carmeliet J. Uncertainty and global sensitivity analysis for the optimal design of distributed energy systems. Appl Energy 2018;214:219–38. http://dx.doi.org/10.1016/j.apenergy.2018.01.062.

[9] Woods DD. Four concepts for resilience and the implications for the future of resilience engineering. In: Special issue on resilience engineering, Reliab Eng Syst Saf In: Special issue on resilience engineering, 2015;141:5–9.http://dx.doi.org/10.1016/j.ress.2015.03.018,

[10] Majewski D, Wirtz M, Lampe M, Bardow A. Robust multi-objective optimization for sustainable design of distributed energy supply systems. Comput Chem Eng 2017;102:26–39. http://dx.doi.org/10.1016/j.compchemeng.2016.11.038.

[11] Mavromatidis G, Orehounig K, Carmeliet J. Comparison of alternative decision-making criteria in a two-stage stochastic program for the design of distributed energy systems under uncertainty. Energy 2018;156:709–24. http://dx.doi.org/10.1016/j.energy.2018.05.081.

[12] Pazouki S, Haghifam M-R. Optimal planning and scheduling of energy hub in presence of wind, storage and demand response under uncertainty. Int J Electr Power Energy Syst 2016;80:219–39. http://dx.doi.org/10.1016/j.ijepes.2016.01.044.

[13] Afzali SF, Cotton JS, Mahalec V. Urban community energy systems design under uncertainty for specified levels of carbon dioxide emissions. Appl Energy 2020;259:114084. http://dx.doi.org/10.1016/j.apenergy.2019.114084.

[14] Balderrama S, Lombardi F, Riva F, Canedo W, Colombo E, Quoilin S. A two-stage linear programming optimization framework for isolated hybrid microgrids in a rural context: The case study of the "El Espino" community. Energy 2019;188:116073. http://dx.doi.org/10.1016/j.energy.2019.116073.

[15] Martínez Ceseña EA, Mancarella P. Energy systems integration in smart districts: robust optimisation of multi-energy flows in integrated electricity, heat and gas networks. IEEE Trans Smart Grid 2019;10(1):1122–31. http://dx.doi.org/10.1109/TSG.2018.2828146.

[16] Tanaka I, Yuge H, Ohmori H. Formulation and evaluation of long-term allocation problem for renewable distributed generations. IET Renew Power Gener 2017;11(12):1584–96. http://dx.doi.org/10.1049/iet-rpg.2017.0068.

[17] Majewski DE, Lampe M, Voll P, Bardow A. TRusT: A Two-stage Robustness Trade-off approach for the design of decentralized energy supply systems. Energy 2017;118:590–9. http://dx.doi.org/10.1016/j.energy.2016.10.065.

[18] Akbari K, Jolai F, Ghaderi S. Optimal design of distributed energy system in a neighborhood under uncertainty. Energy 2016;116:567–82. http://dx.doi.org/10.1016/j.energy.2016.09.083.

[19] Pickering B, Choudhary R. District energy system optimisation under uncertain demand: handling data-driven stochastic profiles. Appl Energy 2019;236:1138–57. http://dx.doi.org/10.1016/j.apenergy.2018.12.037.

[20] Zatti M, Martelli E, Amaldi E. A three-stage stochastic optimization model for the design of smart energy districts under uncertainty. In: Espuña A, Graells M, Puigjaner L, editors. Computer aided chemical engineering. 27 European symposium on computer aided process engineering, vol. 40, Elsevier; 2017, p. 2389–94. http://dx.doi.org/10.1016/B978-0-444-63965-3.50400-1.

[21] Li Z, Ding R, Floudas CA. A comparative theoretical and computational study on robust counterpart optimization: I. robust linear optimization and robust mixed integer linear optimization. Ind Eng Chem Res 2011;50(18):10567–603. http://dx.doi.org/10.1021/ie200150p.

[22] Zhou Y, Wei Z, Sun G, Cheung KW, Zang H, Chen S. A robust optimization approach for integrated community energy system in energy and ancillary service markets. Energy 2018;148:1–15. http://dx.doi.org/10.1016/j.energy.2018.01.078.

[23] Vahid-Pakdel MJ, Nojavan S, Mohammadi-ivatloo B, Zare K. Stochastic optimization of energy hub operation with consideration of thermal energy market and demand response. Energy Convers Manage 2017;145:117–28. http://dx.doi.org/10.1016/j.enconman.2017.04.074.

[24] Mavromatidis G, Orehounig K, Carmeliet J. Design of distributed energy systems under uncertainty: A two-stage stochastic programming approach. Appl Energy 2018;222:932–50. http://dx.doi.org/10.1016/j.apenergy.2018.04.019.

[25] Bruninx K, Delarue E. Scenario reduction techniques and solution stability for stochastic unit commitment problems. In: 2016 IEEE international energy conference. 2016, p. 1–7. http://dx.doi.org/10.1109/ENERGYCON.2016.7514074.

[26] Bucciarelli M, Paoletti S, Vicino A. Optimal sizing of energy storage systems under uncertain demand and generation. Appl Energy 2018;225:611–21. http://dx.doi.org/10.1016/j.apenergy.2018.03.153.

[27] Good N, Mancarella P. Flexibility in multi-energy communities with electrical and thermal storage: A stochastic, robust approach for multi-service demand response. IEEE Trans Smart Grid 2017;PP(99):1. http://dx.doi.org/10.1109/TSG.2017.2745559.

[28] Conejo AJ, Carrión M, Morales JM. Decision making under uncertainty in electricity markets, vol. 1. Springer; 2010.

[29] Gabrielli P, Fürer F, Mavromatidis G, Mazzotti M. Robust and optimal design of multi-energy systems with seasonal storage through uncertainty analysis. Appl Energy 2019;238:1192–210. http://dx.doi.org/10.1016/j.apenergy.2019.01.064.

[30] Pickering B, Choudhary R. Mitigating risk in district-level energy investment decisions by scenario optimisation. In: Proceedings of BSO 2018. 2018, p. 38–45.
[31] Pfenninger S, Staffell I. Long-term patterns of European PV output using 30 years of validated hourly reanalysis and satellite data. Energy 2016;114:1251–65. http://dx.doi.org/10.1016/j.energy.2016.08.060.
[32] Pfenninger S. Dealing with multiple decades of hourly wind and PV time series in energy models: A comparison of methods to reduce time resolution and the planning implications of inter-annual variability. Appl Energy 2017;197:1–13. http://dx.doi.org/10.1016/j.apenergy.2017.03.051.
[33] Kotzur L, Markewitz P, Robinius M, Stolten D. Impact of different time series aggregation methods on optimal energy system design. Renew Energy 2018;117:474–87. http://dx.doi.org/10.1016/j.renene.2017.10.017.
[34] Pfenninger S, Pickering B. Calliope: A multi-scale energy systems modelling framework. J Open Sour Softw 2018;3(29):825. http://dx.doi.org/10.21105/joss.00825.
[35] Mavromatidis G, Orehounig K, Carmeliet J. Uncertainty and global sensitivity analysis for the optimal design of distributed energy systems. Appl Energy 2018;214:219–38. http://dx.doi.org/10.1016/j.apenergy.2018.01.062.
[36] Gabrielli P, Gazzani M, Martelli E, Mazzotti M. Optimal design of multi-energy systems with seasonal storage. Appl Energy 2018;219:408–24. http://dx.doi.org/10.1016/j.apenergy.2017.07.142.
[37] Zhang D, Evangelisti S, Lettieri P, Papageorgiou LG. Optimal design of CHP-based microgrids: Multiobjective optimisation and life cycle assessment. Energy 2015;85:181–93. http://dx.doi.org/10.1016/j.energy.2015.03.036.
[38] Hourcade J-C, Pryadarshi S, La Rovere E, Dhar S, Espagne E, Finon D, Pereira A, Pottier A. How to use SVMAs to reduce the Carbon Pricing and Climate Finance Gap: Numerical illustrations. In: How to use svmas to reduce the carbon pricing and climate finance gap: numerical illustrations. 2017.
[39] Brivio C, Moncecchi M, Mandelli S, Merlo M. A novel software package for the robust design of off-grid power systems. J Cleaner Prod 2017;166:668–79. http://dx.doi.org/10.1016/j.jclepro.2017.08.069.
[40] Mandelli S, Brivio C, Colombo E, Merlo M. A sizing methodology based on Levelized Cost of Supplied and Lost Energy for off-grid rural electrification systems. Renew Energy 2016;89:475–88. http://dx.doi.org/10.1016/j.renene.2015.12.032.
[41] Bukhsh WA, Papakonstantinou A, Pinson P. A robust optimisation approach using CVaR for unit commitment in a market with probabilistic offers. In: 2016 IEEE international energy conference. 2016, p. 1–6. http://dx.doi.org/10.1109/ENERGYCON.2016.7514076.
[42] Gangopadhyay A, Sampath A, Velury B, Sen Gupta D, Ahuja D. Wind and solar energy for reducing electricity deficits in karnataka. Current Sci 2016;111(5):796–807. http://dx.doi.org/10.18520/cs/v111/i5/796-807.
[43] Khodabakhsh R, Sirouspour S. Optimal control of energy storage in a microgrid by minimizing conditional value-at-risk. IEEE Trans Sustain Energy 2016;7(3):1264–73. http://dx.doi.org/10.1109/TSTE.2016.2543024.
[44] Jin M, Feng W, Marnay C, Spanos C. Microgrid to enable optimal distributed energy retail and end-user demand response. Appl Energy 2018;210:1321–35. http://dx.doi.org/10.1016/j.apenergy.2017.05.103.
[45] Verrilli F, Srinivasan S, Gambino G, Canelli M, Himanka M, Vecchio CD, Sasso M, Glielmo L. Model predictive control-based optimal operations of district heating system with thermal energy storage and flexible loads. IEEE Trans Autom Sci Eng 2017;14(2):547–57. http://dx.doi.org/10.1109/TASE.2016.2618948.
[46] Giraud L, Merabet M, Baviere R, Vallée M. Optimal control of district heating systems using dynamic simulation and mixed integer linear programming. In: Proceedings of the 12th international modelica conference. Linköping University Electronic Press; 2017, p. 141–50.
[47] Kopanos GM, Georgiadis MC, Pistikopoulos EN. Scheduling energy cogeneration units under energy demand uncertainty. In: 7th IFAC conference on manufacturing modelling, management, and control, IFAC Proc Vol In: 7th IFAC conference on manufacturing modelling, management, and control, 2013;46(9):1280–5.http://dx.doi.org/10.3182/20130619-3-RU-3018.00275,
[48] Megiddo N. On the complexity of linear programming. IBM Thomas J. Watson Research Division; 1986.
[49] Alderson DL, Doyle JC. Contrasting views of complexity and their implications for network-centric infrastructures. IEEE Trans Syst Man Cybern A 2010;40(4):839–52. http://dx.doi.org/10.1109/TSMCA.2010.2048027.
[50] Read D. Some observations on resilience and robustness in human systems. Cybern Syst: Int J 2005;36(8):773–802.
[51] cBalance Solutions. GHG inventory report for electricity generation and consumption in India. White Paper. cBalance Solutions Pvt. Ltd; 2012.
[52] Ltd. BESC. 15th Annual report. Financial Report BESCOM/BC-4/CS/AGM/2017-18/F-22/1044-1066. Bangalore, India; 2017.
[53] Jafari A, Khalili T, Ganjehlou HG, Bidram A. Optimal integration of renewable energy sources, diesel generators, and demand response program from pollution, financial, and reliability viewpoints: A multi-objective approach. J Cleaner Prod 2020;247:119100. http://dx.doi.org/10.1016/j.jclepro.2019.119100.
[54] Omu A, Rysanek A, Stettler M, Choudhary R. Economic, climate change, and air quality analysis of distributed energy resource systems. Procedia Comput Sci 2015;51:2147–56. http://dx.doi.org/10.1016/j.procs.2015.05.487.
[55] Su Y, Kern JD, Characklis GW. The impact of wind power growth and hydrological uncertainty on financial losses from oversupply events in hydropower-dominated systems. Appl Energy 2017;194:172–83. http://dx.doi.org/10.1016/j.apenergy.2017.02.067.
[56] Lombardi F, Pickering B, Colombo E, Pfenninger S. Policy decision support for renewables deployment through spatially explicit practically optimal alternatives. Joule 2020. http://dx.doi.org/10.1016/j.joule.2020.08.002.
[57] Chowdhury AFMK, Dang TD, Bagchi A, Galelli S. Expected benefits of laos' hydropower development curbed by hydroclimatic variability and limited transmission capacity: opportunities to reform. J Water Resour Plann Manage 2020;146(10):05020019. http://dx.doi.org/10.1061/(ASCE)WR.1943-5452.0001279.
[58] Ohlendorf N, Schill W-P. Frequency and duration of low-wind-power events in Germany. Environ Res Lett 2020;15(8):084045. http://dx.doi.org/10.1088/1748-9326/ab91e9.